30 TW and 33 fs pulses delivered by a Ti:Sa amplifier system seeded with a frequency-doubled fiber laser

Simon Boivinet, Alain Pellegrina, Lucas Ranc, Thomas Morbieu, Sébastien Vidal, Jean-Paul Yehouessi, Philippe Morin, Hugo Lecommandoux, Kevin Robin, Cyril Vinçont, et al.

30 TW and 33 fs pulses delivered by a Ti:Sa amplifier system seeded with a frequency-doubled fiber laser

Simon Boivinet,[1] Alain Pellegrina,[2,*] Lucas Ranc,[2,3] Thomas Morbieu,[2] Sébastien Vidal,[1] Jean-Paul Yehouessi,[1] Philippe Morin,[1] Hugo Lecommandoux,[1] Kevin Robin,[1] Cyril Vinçont,[1] Christophe Pierre,[1] Michaël Berisset,[1] Guillaume Machinet,[1] Alexandre Loulier,[1] Johan Boullet,[1] Hervé Besaucele,[2] Benoit Beaurepaire,[2] Olivier Casagrande,[2] Christophe Simon-Boisson,[2] Sébastien Laux,[2] and Sandrine Ricaud[2]

[1]*Centre Technologique Optique et Laser ALPhANOV, 33400 Talence, France*
[2]*THALES LAS France, Laser Solutions Unit, 2 Avenue Gay-Lussac, 78995 Elancourt Cedex, France*
[3]*Laboratoire Charles Fabry, Institut d'Optique, CNRS, University Paris Saclay, Palaiseau, France*
**Corresponding author: alain.pellegrina@fr.thalesgroup.com*

We report a full experimental comparison study on the injection of a Ti:Sa multi-terawatt amplifier chain with a standard 15 fs Ti:Sa oscillator and 35 fs frequency-doubled fiber oscillator. The study highlights that the Ti:Sa oscillator, with high performance in terms of pulse duration and spectral width, can be replaced by the frequency-doubled fiber oscillator to seed Ti:Sa amplifier chains almost without any compromise on the output pulse duration and picosecond contrast. Finally, we demonstrate for the first time to our knowledge a 30 TW and 33 fs Ti:Sa amplifier injected by a fiber oscillator.

1. INTRODUCTION

Electron and ion sources constitute invaluable tools in numerous scientific fields, including medicine [1], chemistry [2], and non-invasive inspection [3]. The free-electron laser (FEL) is one of the well-known electron sources due to its very high versatility in term of wavelength. Indeed, it can cover from microwave to x-rays. However, facilities hosting a FEL have a kilometer scale due the requirement of an electron accelerator usually ensured by synchrotrons. The most promising alternative to well-established electron acceleration as well as electron sources is laser-driven plasma on gas or solid targets. The laser creates and resonantly controls plasma, trapping electrons which are accelerated and simultaneously gain in energy [4,5]. With this method, the size of the electron and ion sources and accelerator may be shrunk and can be less expensive.

To drive plasmas with the right parameters, the required laser should deliver pulses with duration below 35 fs and peak power of at least few tens of terawatts [6]. However, in the field of physics, these two pulse parameters are not the unique criteria. The pulse contrast is also a crucial parameter; it describes how fast the intensity temporally rises and the level of intensity before the pulse. Particle acceleration from a solid target can be severely affected or prevented by a poor pulse contrast. Indeed, it has been shown that it can lead to a deformation and pre-ionization of the target [7,8]. A high contrast is also necessary when the laser pulse is interacting with a gaseous target to avoid uncontrolled plasma evolution due to pre-ionization [9].

Given their characteristics, lasers based on titanium sapphire (Ti:Sa) crystal are exceptional candidates for high-intensity laser chains. Indeed, their large emission cross-section bandwidth and high optical gain allow us to generate ultrashort pulses and amplify them via multi-pass designs. Furthermore, the mature industrial process of large-aperture crystals enables them to reach very high pulse energy. Thanks to these advantages and the technical progress made over the last decade on Ti:Sa-based laser chains [10,11], 10 PW peak power has been demonstrated [10]. Generating sub-35 fs pulses and amplifying them up to a few joules is routinely done by several Ti:Sa laser manufacturers, and these pulse parameters are now accessible for all scientific facilities. Nevertheless, due to its lack of compactness and high cost, the technology faces issues entering the industrial market. With this in mind, a frequency-doubled femtosecond erbium-fiber laser had been proposed by Herda and Zach as a competitive alternative to the Ti:Sa oscillator [12]. While the

concept is known, to our knowledge, no experimental demonstration has been reported for sub-70 fs pulses so far. This may be because all the solutions based on this architecture require free-space elements [12], deliver too-low pulse energy [13], or are not designed with PM fiber, leading to frequency-doubling instability [14]. To fill the gap, we have developed a new architecture of frequency-doubled all-PM fiber laser delivering 35 fs pulses around 800 nm with an energy of 3.5 nJ [15]. However, the proposed design was complex and the use of three amplifier stages did not make it cost-effective enough. Therefore, we recently proposed an original and simpler design delivering pulses centered at 1595 nm with an energy of 30 nJ and a 35 fs duration [16]. We will briefly describe in the following sections the frequency-doubling stage of this latest architecture.

In this paper, we propose a fully comparative experiment for seeding multi-terawatt (TW) Ti:Sa laser chains using a standard 15 fs Ti:Sa oscillator or our 35 fs long frequency-doubled fiber oscillator. To well compare the impact of the seeder on the output parameters, the amplifier chain design and parameters (such as pump power, number pass in regenerative amplifier, or beam diameters) have been kept identical. This test demonstrates the interchangeability of the two oscillators in a double chirped pulse amplification (CPA) Ti:Sa amplifier system, delivering 30 TW even if the two oscillators deliver different pulse duration, energy, and spectral width. To our knowledge, with pulse duration of 33 fs, this is the first demonstration of a 30 TW class Ti:Sa laser injected by a sub-40 fs frequency-doubled fiber oscillator.

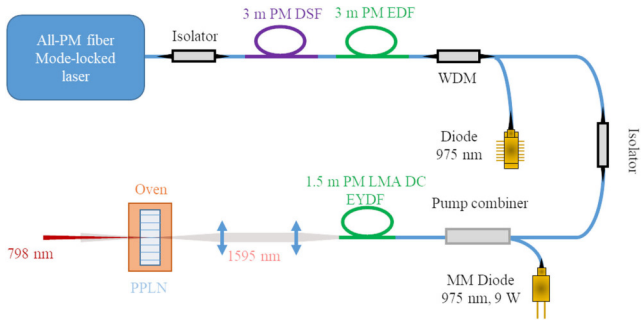

Fig. 1. Schematic of MOPA architecture: DSF, dispersion-compensating fiber; WDM, wavelength-division multiplexer; EDF, erbium doped fiber; LMA DC EYDF, large mode area double clad erbium/ytterbium doped fiber; MMD, multimode diode.

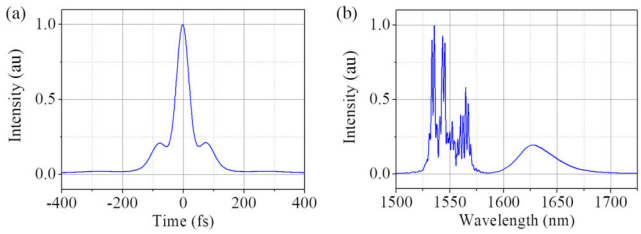

Fig. 2. (a) Autocorrelation trace of the output pulse at the output of the LMA Er/Yb doped amplifier. (b) Optical spectrum at the output of the LMA Er/Yb doped amplifier.

2. FREQUENCY-DOUBLED FIBER LASER

In this Section, we report on the laser architecture of the frequency-doubled fiber oscillator used in the comparative study.

This laser is nearly similar to the one that we recently reported [16]. It is a master oscillator power amplifier (MOPA) design made with only commercially available standard PM fibers (see Fig. 1). The oscillator seeding the amplification chain is a mode-locked laser based on a semiconductor saturable absorber mirror (SESAM) and operating in the solitonic regime. It emits 420 fs long pulses with an energy of 27 pJ at the repetition rate of 40 MHz. At the output of the oscillator, 3 m of dispersion-compensating fiber (DCF) are spliced. Thanks to the normal group velocity dispersion (GVD) of the DCF, the pulses are positively chirped during the propagation. The pulse duration is then 1 ps at the output of the fiber. The nonlinear effects, as self-phase modulation (SPM) along this fiber, broaden the spectrum up to 9 nm. This stretching stage allows us to avoid one normal GVD amplification stage compared to the reported laser in our previous work [15]. The pulses are then amplified through an erbium-doped fiber amplifier (EDFA), which is a backward core-pumped amplifier made with 3 m of doped fiber exhibiting a normal GVD. This amplifier, operating in the parabolic regime, broadens the optical spectrum up to 16 nm and shapes the pulse to seed the last amplifier with the right parameters. This last is based on a PM large mode area (LMA) Er/Yb doped double-clad fiber with anomalous GVD and exhibiting a mode field diameter (MFD) of 20 μm; it is 1.5 m long. While the pulses are amplified, the interplay between nonlinear effect and anomalous GVD lead to a nonlinear compression of the pulses. Due to the large mode field diameter, the energy of the high-order soliton may be higher than standard fiber. The amplified and compressed pulses are finally focused with two lenses into a periodically poled lithium niobate (PPLN) crystal to frequency-double them by second-harmonic generation (SHG). The crystal is inserted in an oven to ensure the temperature stability and temperature-induced phase-matching between the pump and the frequency-doubled signal. The beam diameter is kept larger than 80 μm in order to avoid any intensity-induced damage (beyond 60 GW/cm^2). The large spot size and the large size of the clear aperture of the grating structure in the PPLN (1×1 mm^2) lead to large tolerance for the alignment of the SHG stage.

In our previous work [16], the pulses present large pedestal and satellite pulses due to nonlinear phenomena occurring along the fiber. However, the initial temporal contrast is crucial for the temporal contrast of the Ti:Sa amplifier chain. Keeping this in mind, the pump power of both fiber amplifiers is judiciously controlled to optimize the temporal shape minimizing the pedestal. The resulting pulse energy is only 10 nJ, and the pulses are 39 fs long [see Fig. 2(a)]. The optical spectrum is centered around 1595 nm.

At the output of the SHG stage, the signal average power is 100 mW, corresponding to a pulse energy of 2.5 nJ and a conversion efficiency greater than 25%. The optical spectrum exhibits a large FWHM of 28.8 nm centered at 798 nm [see Fig. 3(a)]. The pulses are linearly chirped with a duration of around 79 fs [see blue curve in Fig. 3(b)]. This chirp is induced by the chromatic dispersion of the optics, as lenses, used to

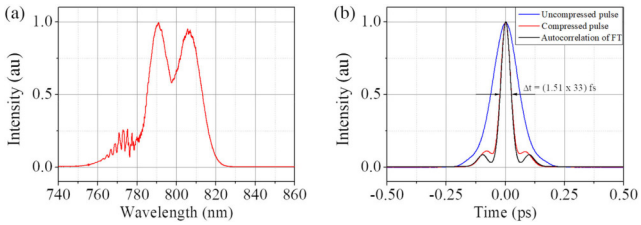

Fig. 3. (a) Optical spectrum from frequency-doubled fiber oscillator. (b) Autocorrelation traces of the uncompressed (blue curve) and compressed (red curve) pulses from the frequency-doubled fiber oscillator and the Fourier transform of the spectrum (black curve).

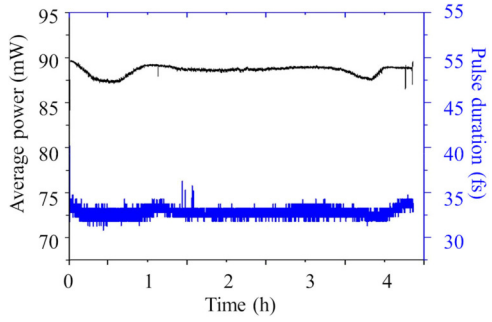

Fig. 4. Time average power (black curve) and pulse duration (blue curve) stability measurement over about 4 h.

collimate the frequency-doubled signal or the PPLN crystal (having a GVD around 300 fs^2/mm). However, they are compressible down to 33 fs via paired SF10-prism compressors [see red curve in Fig. 3(b)]. The compressed pulses are nearly Fourier transform-limited because the autocorrelation trace of the Fourier transform of the spectrum, assuming a null spectral phase [see black curve in Fig. 3(b)], is almost overlapping the experimental autocorrelation trace. The trace has small femtosecond pedestal arising from the oscillating spectral shape. We assume this is driven by the shape of the optical spectrum. Indeed, the autocorrelation trace of the Fourier transform of the spectrum also has some pedestals. We have optimized the laser parameters to reach the highest pulse energy and the shortest pulse duration, and to minimize the pedestal.

We have investigated the stability of the pulse durations of the compressed pulse and the average power simultaneously (see Fig. 4). To do this, we have split the signal in two via a non-polarization beam-splitter with a ratio of 10/90. The two parameters have been monitored over 4 h. The average power has a root mean square (RMS) below 0.9%, and the fluctuation of pulse duration is +/− 1.2 fs RMS. These are the same magnitude orders to the stability of Ti:Sa oscillator. It should be noted that we have also proved experimentally in Section 3 that the stability of the amplifier remains the same.

We believe that the interplay between the fiber laser architecture, the limited number of free space optics (only four bulk elements) limiting risk of misalignment, and the optical design features such as tolerances (large clear aperture of PPLN crystal compared to input beam diameter) may help to make the laser robust and probably stable over the long term. These features may improve the reliability of the overall system and reduce the maintenance and service. This maintenance time is also reduced considering that the fiber oscillator does not require any water cooling system (as such system needs to be periodically purged and its filters need to be changed).

It should be noted that the pulse compressor is not used in the rest of the comparison experiment. Indeed, the tool compressor has been set to test pulse compression at oscillator output, but is not yet integrated in the oscillator box. However, the compressor of the Ti:Sa laser chain can be optimized to compensate for the part of the GVD generated by the oscillator.

3. COMPARATIVE STUDY OF THE AMPLIFICATION OF Ti:Sa AND FIBER OSCILLATORS

In this Section, we compare the results obtained at the output of Ti:Sa amplifier chain when a standard seeder (a Ti:Sa oscillator) is interchanged with a frequency-doubled fiber oscillator. To study only the impact of the seeder change, all the other parameters should remain exactly the same (only swap of the oscillators).

Our study has been performed on a standard QUARK 30 TW laser system from Thales. This system is based on a double CPA architecture using a cross-polarization wave (XPW) filter to improve picosecond contrast, as presented in Fig. 5.

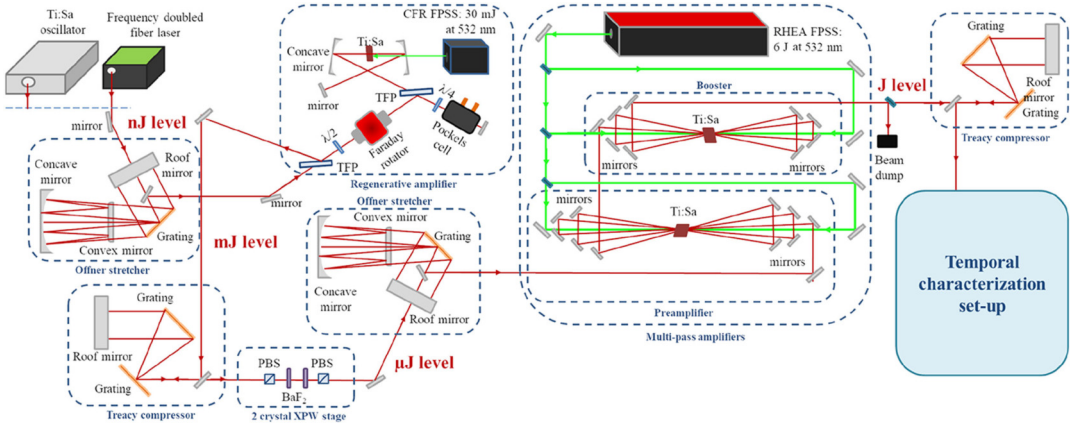

Fig. 5. Global synoptic of the 30 TW double CPA architecture using XPW filter.

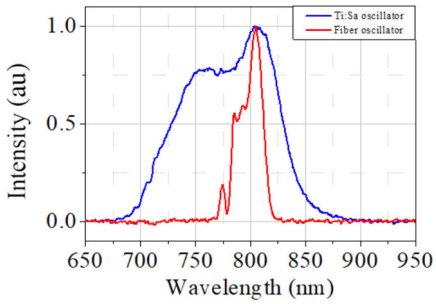

Fig. 6. Optical spectra from the Ti:Sa and fiber oscillators.

Advantageously, XPW nonlinear effect [17] broadens the spectrum to reach pulse durations shorter than 35 fs at the end of the amplifier chain.

The first stage of our system is the pulse generation ensured by a femtosecond mode-locked oscillator. For the study, we used a Gecco Ti:Sa oscillator from Laser Quantum (hereafter called Ti:Sa oscillator), or a frequency-doubled fiber laser co-developed between ALPhANOV and Thales (hereafter called fiber oscillator). The Ti:Sa oscillator delivers pulses at the repetition rate of 80 MHz with a duration compressible down to 15 fs and an energy of 7.5 nJ. Its spectral full width at half maximum (FWHM), recorded with an USB 2000+ spectrometer from Ocean Optics (with a spectral resolution of 0.1 nm), is 103 nm (see blue optical spectrum in Fig. 6). The performance of the fiber oscillator is discussed in the previous part. It should be noted that the laser parameters are slightly different from the ones reported previously. We have lightly adjusted the pump power of the fiber oscillator to reach the largest optical spectrum at the output of the XPW stage. The resulting pulse duration is now 35 fs, but the pulse energy is conserved. The shape of the spectrum has slightly changed (see red curve in Fig. 6), but the FWHM is still 28 nm, almost four times narrower than that delivered by the Ti:Sa oscillator (see Fig. 6). The delivered pulses are linearly chirped at the output of the laser and exhibit a duration of around 79 fs. This chirp is induced by the chromatic dispersion of the optics (as lenses to collimate the frequency-doubled signal). However, we can compress them down to 35 fs. The compressed pulses have a small femtosecond pedestal arising from the oscillating spectral shape. In this study, we do not compress them because it is not required to seed the fs laser chain. It should be mentioned that the fiber oscillator is almost four times smaller, in terms of footprint on the optical breadboard, than the Ti:Sa oscillator (a reduced footprint of 30×15 cm^2 for the optical head instead of 65×28.5 cm^2), and it does not require any water cooling. These two features are for sure very attractive arguments for microscopy applications, but this is also not negligible for the Ti:Sa amplifier. The overall footprint of the QUARK system can be reduced by at least 3.5%. This is for sure not a drastic improvement but still a first step to shrink a bulky system.

The first CPA is composed of an Offner stretcher, a regenerative cavity pumped by a Flash Pump Solid State (FPSS) laser emitting at 532 nm, and a compressor in a Treacy configuration. The spatial beam profile is Gaussian thanks to the regenerative cavity. The amplifier brings the pulse energy from few nanojoules to the millijoule level. This 60 dB gain leads to a spectral narrowing of the seeded pulses and defines the amplification bandwidth (around 30 nm). Therefore, the spectrum of the amplified pulses for the Ti:Sa oscillator is shaped by the amplifier and acquires a Gaussian shape with a bandwidth of 30 nm. The pulses are then only compressible down to 35 fs, limited by the amplification bandwidth of the regenerative cavity. The spectrum of the fiber oscillator almost keeps its shape, but it also experiences a narrowing down to 20 nm. Its compressed pulse duration is increased up to 45 fs.

The compressed pulse is then injected in a two BaF_2 crystal configuration XPW filter [18,19] operating under a lab environment, ensuring reliability and robustness compared to a single-crystal setup. Contrast is improved by 3 orders of magnitude, which is the extinction ratio of the polarizer cube used for the setup. In addition, the spectrum is broadened by a factor of $\sqrt{3}$ and the phase exiting XPW is flat [20]. The spectra obtained from XPW output, shown in Fig. 7(a), are very similar, at 40.4 and 41.5 nm large for the Ti:Sa and fiber oscillator, respectively. However, the spectrum from the Ti:Sa oscillator exhibits larger wings at -10 dB. This should help to recompress the pulse to a shorter duration, and it may also limit the gain narrowing along the last amplification stage. The large spectrum obtained with the fiber oscillator at the output of the XPW stage is almost Gaussian in shape, highlighting a good temporal and phase quality of the seeded pulses (the first CPA stage does not usually induce phase distortion). Indeed, if the pulses had a distorted temporal phase, then the resulting spectrum would not have been a Gaussian shape and would be narrow. To evaluate the long-term stability of the first CPA with the fiber oscillator (the stability with Ti:Sa oscillator is already well-known), we have processed to three spectral measurements spaced two hours apart at the output of the XPW stage during the continuous operation [see Fig. 7(b)]. It is interesting to check the spectral evolution at this point of the amplifier chain because the XPW process is a highly nonlinear process. Any change in terms of temporal phase or spectral shape of the seeded or amplified pulses will lead to a high spectral variation at the output of the XPW stage. The spectra reported in Fig. 7(b) do not exhibit large variation and the spectral shape is conserved. To evaluate the spectral intensity evolution at each wavelength with time, we subtract the initial spectral intensity on each point by the spectral intensity after a given time and divide the initial spectral intensity. The variation of the overall spectrum is around 20%. The spectral intensity variations are not very high considering that the XPW process is a highly nonlinear process enhancing noise, and that the measurement error from the spectrometer is around 10%. Furthermore, the XPW stability behavior is very similar to the one observed with a Ti:Sa oscillator (i.e., spectral intensity variations are below 20%). Therefore, we consider that the first stage of the system seeded by the fiber oscillator is stable enough to seed the second CPA stage.

The second CPA is exclusively based on multi-pass amplifiers in order to reach high gain of more than 40 dB combined with high pulse energy while avoiding pre-pulses generated by cavities. Pulses are stretched again using an Offner stretcher, and amplified through a five-pass pre-amplifier followed by a saturated four-pass amplifier. These amplifiers are pumped by 3 J at 532 nm from an attenuated RHEA 6 J FPSS laser from Thales. Before compression, the last amplifier delivers 1.33 J

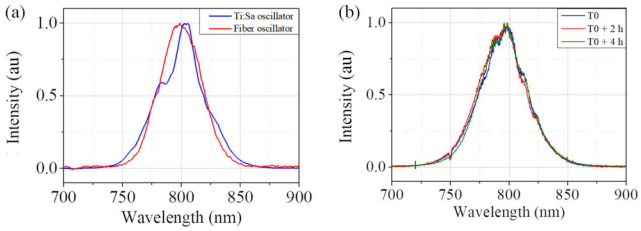

Fig. 7. (a) Spectrum from XPW two-crystal setup. (b) Spectra from XPW two-crystal setup with the fiber oscillator over 4 h.

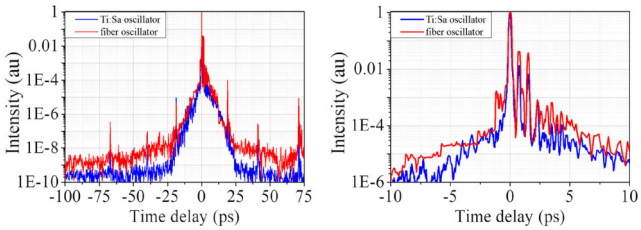

Fig. 9. Third-order correlation trace of the amplified signal from the Ti:Sa and fiber oscillators with two different temporal scales obtained with the same measurement.

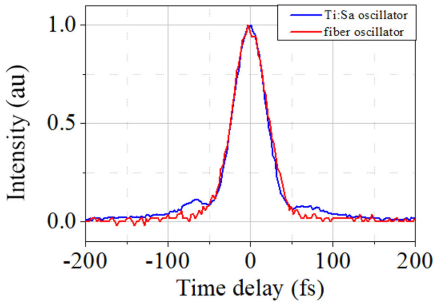

Fig. 8. Autocorrelation trace of the amplified signal from Ti:Sa and fiber oscillators.

with energy fluctuations smaller than 1% rms. A sampling system (using uncoated fused silica wedges) allows us to seed a Treacy compressor operating under air to perform full characterization of the beam. Pulse duration measurements have been realized using a TAIGA second-order auto-correlator from Thales. Figure 8 illustrates the autocorrelation trace of the compressed pulses. Autocorrelation of the pulse from the Ti:Sa oscillator is 46.3 fs FWHM. With the fiber oscillator, we obtained duration of 48.6 fs FWHM. Assuming a sech^2 shape, it gives pulse duration of 30.6 fs with the Ti:Sa oscillator and 32.3 fs with the fiber oscillator. It is important to mention that no acousto-optic programmable dispersive filter (AOPDF) has been used to optimize compression, explaining the wings on autocorrelation using the Ti:Sa oscillator. It should be also noted that the final pulse duration with the fiber oscillator is shorter than the seeded one, and it no longer has any pedestal femtosecond thanks to the use of XPW stage.

The measured efficiency of our compressor, including gratings (with efficiency higher than 93%), is equal to 75%. The resulting peak power for both oscillators is then 30 TW. To the best of our knowledge, we demonstrate a higher peak power and the shortest pulse duration delivered by an amplifier system seeded with a frequency-doubled fiber oscillator.

In most particle-acceleration experiments such as laser-driven ion acceleration, the ultra-short pulse duration necessary to reach high peak power is not the unique criteria. Indeed, the pulse contrast is also a crucial parameter. To evaluate this last parameter, we proceed to picosecond contrast measurements with a TUNDRA third-order auto-correlator from Ultrafast Innovation. Its noise level has been measured below $1{:}10^{11}$ for all measurements by shutting the fundamental and then SHG signal. Figure 9 shows cross-correlation of pulses from both oscillators. We can consider in the first instance that the cross-correlation traces are quite similar. The pre-pulse peaks at 66, 40, and 18 ps are well known post-pulse replicas coming from tool compressor and diagnostic bench; hence their presence on both Ti:Sa and fiber oscillator third-order correlation traces. Indeed, similar post pulse at −66, −40, and −18 ps with intensity difference of an order of magnitude are also observed. The replicas are not related to cross-correlation measurement, and they can be avoided with the use of a new compressor tool. It is important to mention that no other pre-pulses are observed; this was not self-evident due to the all-PM design, which may lead to some pulse replicas [21]. Amplified spontaneous emission (ASE) of the system before hundreds of picoseconds is kept below 10^{-8}. The contrast from −50 to −25 ps is below 10^{-7} for the two oscillators. The Ti:Sa oscillator contrast is almost 1 order of magnitude lower than that of the fiber oscillator. The differences in term of ASE contrast may arise from the laser design. Indeed, the architecture of the fiber oscillator is based on concatenation of nonlinear amplifiers [15,16] generating ASE because they are designed to pulse-shape ultra-short pulses at the expense of the contrast ratio. While SHG suppress some of picosecond background, it does not remove it totally. However, the contrast is perfect for gaseous targets requiring a contrast better than 10^{-6} for a Joule class laser. It is also good enough for solid targets usually requiring a 10^{-9} contrast without any pre-pulse. For the contrast from −20 to 20 ps, there are also some differences but they are smaller than 1 order of magnitude. As is it coherent contrast, we assume that these slight differences might be partially corrected by the use of an AOPDF.

4. CONCLUSION

In conclusion, we have proven that a standard Ti:Sa oscillator with high performance in terms of energy, pulse duration, and spectral width can be replaced by a compact 35 fs frequency-doubled fiber oscillator to seed a Ti:Sa amplifier chain without almost any compromise on the output pulse duration, and with only a small degradation of 1 order of magnitude on the picosecond contrast. Moreover, we have demonstrated for the first time to our knowledge that sub-35 fs pulses with a peak power of 30 TW can be achieved with a frequency-doubled fiber laser seeding a standard Ti:Sa amplifier chain. This means that these kinds of fiber oscillators can compete with Ti:Sa oscillators while being smaller, cheaper, and more robust and reliable than the solid-state lasers. The table top (1.5 m × 4.5 m) double CPA architecture, using robust solutions such as two-crystal XPW under air and well-established, highly reliable fiber oscillators, is

paving the way to the rugged and hands-free multi-TW systems necessary for laser plasma-based electron or ion sources.

Disclosures. The authors declare no conflicts of interest.

REFERENCES

1. J. B. Pełka, K. R. Tybor, R. Nietubyc, and G. Wrochna, "Applications of free electron lasers in biology and medicine," Acta Phys. Pol. A **1178553**, 427–432 (2010).
2. J. Möller, M. Sprung, A. Madsena, and C. Gutt, "X-ray photon correlation spectroscopy of protein dynamics at nearly diffraction-limited storage rings," IUCrJ **6**, 794–803 (2019).
3. C. Behrens, F. Decker, Y. Ding, V. A. Dolgashev, J. Frisch, Z. Huang, P. Krejcik, H. Loos, A. Lutman, T. J. Maxwell, J. Turner, J. Wang, M.-H. Wang, J. Welch, and J. Wu, "Few-femtosecond time-resolved measurements of X-ray free-electron lasers," Nat. Commun. **5**, 3762 (2014).
4. M. E. Couprie, "Towards compact free electron–laser based on laser plasma accelerators," Nucl. Inst. Methods Phys. A **909**, 5–15 (2018).
5. J. Faure, B. van der Geer, B. Beaurepaire, G. Gallé, A. Vernier, and A. Lifschitz, "Concept of a laser-plasma-based electron source for sub-10-fs electron diffraction," Phys. Rev. Accel. Beams **19**, 021302 (2016).
6. T. André, I. A. Andriyash, A. Loulergue, M. Labat, E. Roussel, A. Ghaith, M. Khojoyan, C. Thaury, M. Valléau, F. Briquez, F. Marteau, K. Tavakoli, P. N'Gotta, Y. Dietrich, G. Lambert, V. Malka, C. Benabderrahmane, J. Vétéran, L. Chapuis, T. El Ajjouri, M. Sebdaoui, N. Hubert, O. Marcouillé, P. Berteaud, N. Leclercq, M. El Ajjouri, P. Rommeluère, F. Bouvet, J.-P. Duval, C. Kitegi, F. Blache, B. Mahieu, S. Corde, J. Gautier, K. Ta Phuoc, J. P. Goddet, A. Lestrade, C. Herbeaux, C. Évain, C. Szwaj, S. Bielawski, A. Tafzi, P. Rousseau, S. Smartsev, F. Polack, D. Dennetière, C. Bourassin-Bouchet, C. De Oliveira, and M.-E. Couprie, "Control of laser plasma accelerated electrons for light sources," Nat. Commun. **9**, 1334 (2018).
7. O. Lundh, F. Lindau, A. Persson, C.-G. Wahlström, P. McKenna, and D. Batani, "Influence of shock waves on laser-driven proton acceleration," Phys. Rev. E **76**, 026404 (2007).
8. K. Zeil, S. D. Kraft, S. Bock, M. Bussmann, T. E. Cowan, T. Kluge, J. Metzkes, T. Richter, R. Sauerbrey, and U. Schramm, "The scaling of proton energies in ultrashort pulse laser plasma acceleration," New J. Phys. **12**, 045015 (2010).
9. G. S. Sarkisov, V. Y. Bychenkov, V. T. Tikhonchuk, A. Maksimchuk, S. Y. Chen, R. Wagner, G. Mourou, and D. Umstadter, "Observation of the plasma channel dynamics and Coulomb explosion in the interaction of a high-intensity laser pulse with a He gas jet," J. Exp. Theor. Phys. Lett. **66**, 828–834 (1997).
10. F. Lureau, G. Matras, S. Laux, C. Radier, O. Chalus, O. Casagrande, C. Derycke, S. Ricaud, P. Calvet, L. Boudjemaa, C. Simon-Boisson, D. Ursescu, and I. Dancus, "10 PetaWatt laser system for extreme light physics," in *Laser Congress 2019 (ASSL, LAC, LS&C)* (2019), paper ATh1A.5.
11. G. Matras, F. Lureau, S. Laux, O. Casagrande, C. Radier, O. Chalus, F. Caradec, L. Boudjemaa, C. Simon-Boisson, R. Dabu, F. Jipa, L. Neagu, I. Dancus, D. Sporea, C. Fenic, and C. Grigoriu, "First operation above PetaWatt with sub-25 fs pulses," in *Research in Optical Sciences* (2014), paper HTu2C.4.
12. R. Herda and A. Zach, "Generation of 32-fs pulses at 780 nm by frequency doubling the solitonically-compressed output of an Erbium-doped fiber-laser system," in *Conference on Lasers and Electro-Optics* (2012), paper CTh1N.4.
13. J. Sotor and G. Sobon, "24 fs and 3 nJ pulse generation from a simple, all polarization maintaining Er-doped fiber laser," Laser Phys. Lett. **13**, 125102 (2016).
14. J. W. Nicholson, A. D. Yablon, P. S. Westbrook, K. S. Feder, and M. F. Yan, "High power, single mode, all-fiber source of femtosecond pulses at 1550 nm and its use in supercontinuum generation," Opt. Express **12**, 3025–3034 (2004).
15. S. Boivinet, P. Morin, J. P. Yehouessi, S. Vidal, G. Machinet, and J. Boullet, "Sub-50 fs 3.5 nJ pulses at 792 nm generated by frequency doubling of an all-PM fiber laser for Ti:sapphire injection," Proc. SPIE **10897**, 108971J (2019).
16. S. Boivinet, P. Morin, J.-P. Yehouessi, S. Vidal, G. Machinet, and J. Boullet, "1.1 W all-PM fiber laser at 1600 nm delivering 35 fs pulses with 30 nJ energy," in *Laser Congress 2019 (ASSL, LAC, LS&C)* (2019), paper ATh2A.6.
17. A. Jullien, O. Albert, F. Burgy, G. Hamoniaux, J.-P. Rousseau, J.-P. Chambaret, F. Augé-Rochereau, G. Chériaux, J. Etchepare, N. Minkovski, and S. M. Saltiel, "10-10 temporal contrast for femtosecond ultraintense lasers by cross-polarized wave generation," Opt. Lett. **30**, 920–922 (2005).
18. "High contrast non-linear femtosecond pulse filter," Patent application EP1662306 (A1).
19. A. Jullien, J.-P. Rousseau, B. Mercier, L. Antonucci, O. Albert, G. Chériaux, S. Kourtev, N. Minkovski, and S. S. Saltiel, "Highly-efficient nonlinear filter for femtosecond pulse contrast enhancement and pulse shortening," Opt. Lett. **33**, 2353–2355 (2008).
20. L. P. Ramirez, D. N. Papadopoulos, A. Pellegrina, P. Georges, F. Druon, P. Monot, A. Ricci, A. Jullien, X. Chen, J. P. Rousseau, and R. Lopez-Martens, "Efficient cross polarized wave generation for compact, energy-scalable, ultrashort laser sources," Opt. Express **19**, 93–98 (2011).
21. S. Boivinet, "Solutions innovantes pour réaliser des lasers à impulsions ultra-brèves, stables et fiables pour applications industrielles," Ph.D. dissertation (Faculté Polytechnique de Mons, 2016).